Hindawi
Journal of Electrical and Computer Engineering
Volume 2018, Article ID 3579619, 11 pages
https://doi.org/10.1155/2018/3579619

Research Article

Parallel Resampling of OFDM Signals for Fluctuating Doppler Shifts in Underwater Acoustic Communication

Shingo Yoshizawa,[1] **Takashi Saito**,[2] **Yusaku Mabuchi**,[2] **Tomoya Tsukui**,[3] **and Shinichi Sawada**[3]

[1]*Kitami Institute of Technology, Kitami, Japan*
[2]*Mitsubishi Electric TOKKI Systems Corporation, Kamakura, Japan*
[3]*IHI Corporation, Yokohama, Japan*

Correspondence should be addressed to Shingo Yoshizawa; yosizawa@mail.kitami-it.ac.jp

Received 15 June 2018; Revised 22 August 2018; Accepted 9 October 2018; Published 4 November 2018

Academic Editor: Jit S. Mandeep

Reliable underwater acoustic communication is demanded for autonomous underwater vehicles (AUVs) and remotely operated underwater vehicles (ROVs). Orthogonal frequency-division multiplexing (OFDM) is robust with multipath interference; however, it is sensitive to Doppler. Doppler compensation is given by two-step processing of resampling and residual carrier frequency offset (CFO) compensation. This paper describes the improvement of a resampling technique. The conventional method assumes a constant Doppler shift during a communication frame. It cannot cope with Doppler fluctuation, where relative speeds between transmitter and receiver units are fluctuating. We propose a parallel resampling technique that a resampling range is extended by measured Doppler standard deviation. The effectiveness of parallel resampling has been confirmed in the communication experiment. The proposed method shows better performance in bit error rates (BERs) and frame error rates (FERs) compared with the conventional method.

1. Introduction

Autonomous underwater vehicles (AUVs) and remotely operated underwater vehicles (ROVs) are of wide interest for marine survey and offshore engineering. Reliable underwater communication is essential for command control and image/video data transmission. In recent underwater acoustic communication (UAC), orthogonal frequency-division multiplexing (OFDM) is widely used in terms of high-frequency utilization [1]. OFDM inserts a cyclic prefix (CP) or a guard interval (GI) into block data and makes use of frequency domain equalization (FDE) as multipath compensation. We have presented the countermeasure against strong multipath, where a multipath spread exceeds a CP length in [2].

Although OFDM is robust with multipath interference, it is sensitive to Doppler. Due to the low velocity of acoustic waves, the wideband modulation of OFDM is considerably affected by Doppler and results in intercarrier interference (ICI). Doppler compensation is mandatory for moving platforms such as AUVs and ROVs. Doppler compensation is given by two steps of resampling and residual carrier frequency offset (CFO) correction [3, 4]. This paper describes the improvement of a resampling technique.

Doppler is expressed by frequency scaling in narrow band signals. This model is often used in electromagnetic wave communication. In UAC, the wideband model of time scaling (expansion or compression) is assumed when the signal bandwidth is close to carrier frequency. Resampling manipulates a received signal to compensate the time-scale change. The resampling ratio is determined according to the Doppler estimation result observed as the change of signal time length or frequency.

If a Doppler shift is simple and known, Doppler compensation would be perfectly performed by the incorporation of resampling and CFO correction. However, nonuniform Doppler shifts must be considered in actual communication. Nonuniform Doppler shifts are classified into Doppler spread and Doppler fluctuation as shown in Figure 1.

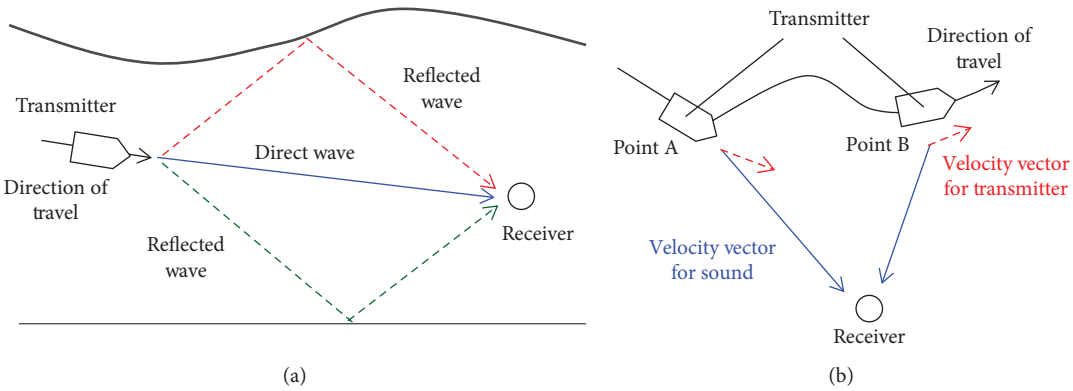

Figure 1: Types of nonuniform Doppler shifts. (a) Doppler spread and (b) Doppler fluctuation.

Doppler spread is caused by the acoustic propagation that each path has an individual Doppler scale factor. In Figure 1(a), the transmitter unit has the same direction as the direct wave. The reflected waves have the different directions, whose Doppler scales are slightly shifted from that of the direct wave. These Doppler scales are measured as frequency spread in the receiver unit. The countermeasures of Doppler spread have been presented in recent papers such as multiple resampling [5], Bayesian resampling [6], frequency domain oversampling [7], and Doppler-resilient orthogonal signal-division multiplexing (D-OSDM) [8].

Doppler fluctuation is caused by the irregular motions of transmitter or receiver units. The case that the transmitter unit is moving in meandering trajectory is depicted in Figure 1(b). A Doppler shift becomes positive in Point A and negative in Point B according to the relation between sound and transmitter velocity vectors. While the Doppler shift in Figure 1(a) is regarded to be time invariant, the Doppler shift in Figure 1(b) rapidly fluctuates with plus or minus as time goes on. There are few papers to tackle Doppler fluctuation because of difficulty in acoustic propagation modeling. The authors in [9] have presented linear multiscale compensation by smoothing estimated Doppler scales. It assumes that a Doppler shift is linearly changing. This paper discusses more severe Doppler fluctuation where a Doppler shift changes with plus or minus. The conventional method assumes a time invariant (or linearly changing) Doppler shift during a communication frame. It cannot cope with severe Doppler fluctuation, where a relative speed between transmitter and receiver units is fluctuating within a communication frame.

This paper presents a parallel resampling technique that a resampling range is extended by measured Doppler dispersion. If an OFDM block is affected by Doppler fluctuation, using Doppler shift average is insufficient for finding an appropriate resampling ratio. We apply statistical analysis that uses both mean and variance in Doppler estimation to cope with complicated Doppler shift variations. The parallel resampling receiver takes multiple resampling blocks whose resampling ratios are settled according to Doppler mean and deviation. The best decoded data are selected by checking data errors. The parallel resampling stricture is applicable to typical OFDM systems. The effectiveness of parallel resampling has been tested by our sea trial, where a transmitter unit moves with various speeds and directions.

A part of contents in this paper has been presented in the conference paper as our previous work [10]. The following two points have been improved in this paper. One is the frequency allocation of a continuous wave (CW) whose signal is given by a sinusoidal function. The previous work requires frequency spacing between CW and OFDM bands to avoid their own interference, which results in low-frequency utilization. This work has improved that CW is allocated as one of the OFDM subcarriers. The signal interference can be avoided by making use of frequency orthogonality of OFDM. The second is the dynamic control of branches in the parallel resampling receiver. The parallel numbers of resampling units are controlled on frame-by-frame basis according to the measured Doppler shift mean and deviation. It can reduce computational complexity of resampling compared with the fixed branches in our previous work.

This paper is organized as follows. Section 2 explains fundamentals of Doppler and resampling and reports examples of Doppler tolerance in OFDM. Section 3 investigates the influence of Doppler fluctuation. Section 4 proposes a parallel resampling technique. Section 5 reports the experimental results in the Doppler test. Section 6 summarizes our work.

2. Resampling

The velocity of acoustic waves (about 1500 m/s underwater) is much lower than that of electromagnetic waves. The effect of Doppler gives a great impact on acoustic communication. The relative Doppler shift Δ is defined as a ratio of source relative velocity to propagation wave velocity. For a single-frequency component f, the Doppler effect is expressed by a frequency scaling:

$$f' = f(1 + \Delta). \tag{1}$$

In wideband signals, each frequency component is affected by a different amount. This Doppler effect is modeled by a time scaling (expansion or compression) of the signal waveform:

$$r(t) = s((1+\Delta)t), \tag{2}$$

where $s(t)$ and $r(t)$ are the source and received signals, repectively. When we use a discrete time-sampled source signal $s[nT_s]$, where n is an integer number and T_s is a sampling period, the received signal is expressed as

$$r[nT_s] = s[(1+\Delta)nT_s]. \tag{3}$$

The rate conversion of $1/(1+\Delta)$, i.e., resampling, eliminates the effect of Doppler by the following equation:

$$r\left[\frac{1}{1+\Delta}nT_s\right] = s[nT_s]. \tag{4}$$

Doppler estimation for resampling is accomplished by inserting a known sequence to a communication frame. A popular approach is to detect the times of arrival of preamble and postamble [11] shown in Figure 2. A Doppler shift can be measured as the change of signal length by $(1+\Delta)LT_s$, where LT_s is the interval between preamble and postamble.

The tolerance for Doppler estimation error can be investigated from a simple OFDM model in Figure 3. The relative Doppler shift is added to a transmit signal. The OFDM parameters of simulation are enumerated in Table 1. These parameters are just one of the examples because adequate OFDM parameters depend on acoustic propagation conditions. The similar parameters have been adopted for our experiment in Section 5.

The results of error vector magnitude (EVM) and bit error rate (BER) are plotted in Figure 4. The horizontal axis shows a Doppler shift corresponding to the residual error of Doppler estimation. A bit error occurs when EVM exceeds 40% when comparing the results in Figures 4(a) and 4(b). Since the center frequency is 45 kHz, a Doppler shift of 4.5 Hz is equivalent to 1/10000 in a relative Doppler shift. It indicates that a resolution of utmost 1/10000 is required within an allowable resampling ratio error. Frequency domain oversampling [7] can extend the error tolerance; however the tolerance is less than 5 Hz. We assume the Doppler deviation of 10 Hz in Doppler fluctuation, which is tested in Section 3. Only applying frequency domain oversampling cannot cope with this large Doppler fluctuation.

3. Influence of Doppler Fluctuation

The influence of Doppler fluctuation is investigated by applying various Doppler shift patterns into an OFDM block. First, we explain our Doppler fluctuation model illustrated in Figure 5, comparing two types of Doppler shift models. The constant Doppler shift model gives the same direction in the sound and transmitter velocity vectors, where a constant Doppler shift of Δ_C is observed. In the Doppler fluctuation model, the direction of a transmitter unit swings during sending one OFDM frame. The Doppler shift changes Δ_C, $\Delta_C + \Delta$, and $\Delta_C - \Delta$ due to the relation between sound and transmitter velocity vectors.

Since the constant component Δ_C can be eliminated by a typical Doppler compensation technique, we consider the

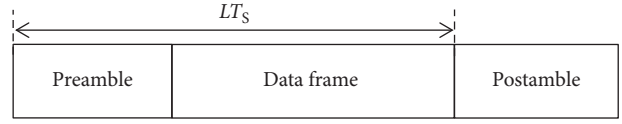

Figure 2: Frame format for Doppler estimation.

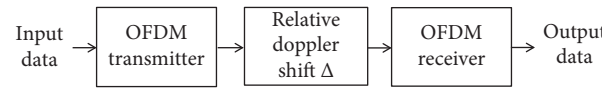

Figure 3: OFDM model with Doppler shift.

Table 1: OFDM parameters.

Modulation	QPSK-OFDM
Sampling frequency (kHz)	200
Center frequency (kHz)	45
Frequency band (kHz)	30 to 60
FFT size	1024
FFT length (ms)	34.1
GI length (ms)	4.3
Number of data subcarriers	512
Number of pilot subcarriers	512
OFDM frame length (ms)	38.4
Frequency domain oversampling factor	1, 2
FEC (coding rate)	Convolutional coding (3/4)
Channel model	AWGN
CNR	30 dB

Doppler shifts of 0, Δ, and $-\Delta$ by applying $\Delta_C = 0$. Figure 6 shows the OFDM block with Doppler shift patterns. One OFDM block with N samples is partitioned into three sections of A, B, and C. We make various Doppler shift patterns by shuffling the Doppler shifts in three sections so that all the shifts are allocated in a whole frame. Although further complex shifts should be considered in the actual environment, the proposed parallel resampling technique can cope with arbitrary unknown Doppler shifts (to be described later). We represent arbitrary shifts by shuffling the three Doppler shifts (expressing the swing of a transmitter unit as one of the examples) for simplification. Our model that a Doppler shift fluctuates with plus or minus in a whole frame can be observed in actual communication, which will be reported in Section 5.

The resampling procedure is illustrated in Figure 7. We evaluate various resampling ratios of $1/(1-\Delta)$, $1/(1-(\Delta/2))$, 1, $1/(1+(\Delta/2))$, and $1/(1+\Delta)$ to observe which ratio is the best choice. The magnitude of Doppler shift is set by $\Delta \cdot f_C = 10$ Hz, assuming the speed fluctuations of $\pm$ 1.2 km/h in moving platforms. f_C(=45 kHz) denotes the center frequency of OFDM. The other simulation parameters are the same in Table 1. The OFDM block sample N becomes 7,740 including the guard interval. The frequency domain oversampling factor of 2 is applied to extend the Doppler tolerance.

The results of EVMs and BERs are shown in Tables 2 and 3. The OFDM block length is the same for all cases. The highlighted cell shows the best performance for each case.

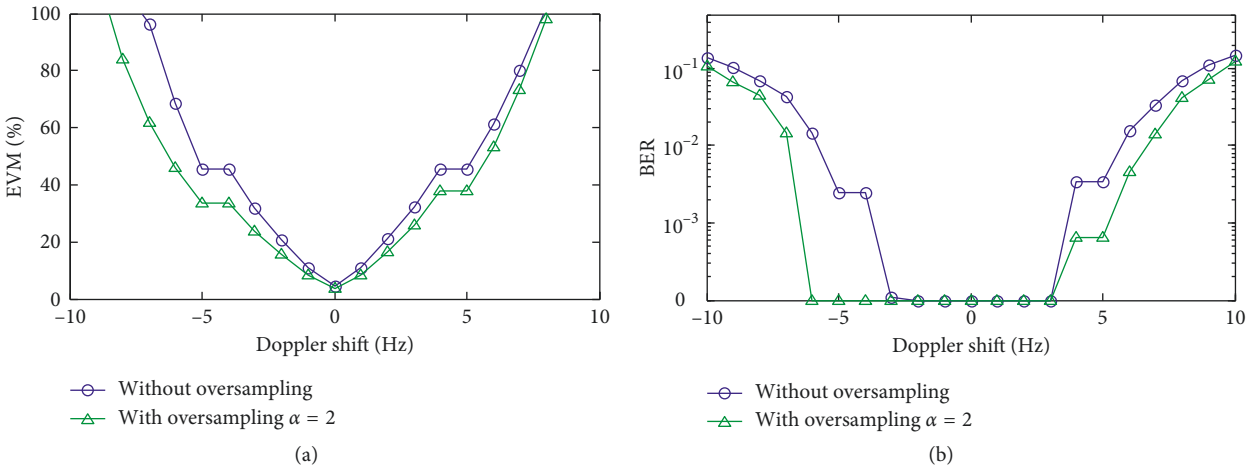

Figure 4: Tolerance for Doppler estimation errors. (a) EVM and (b) BER.

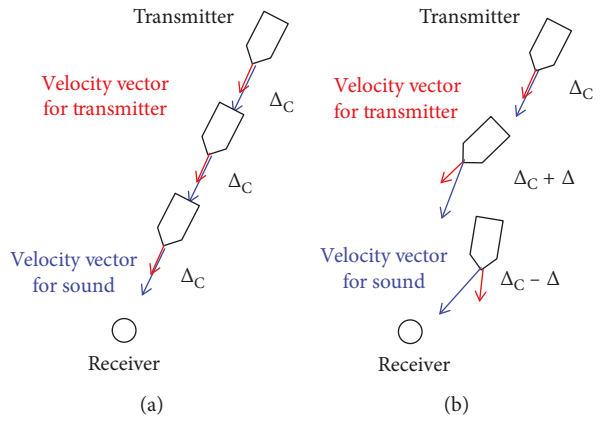

Figure 5: Doppler shift models. (a) Constant Doppler shift and (b) Doppler fluctuation.

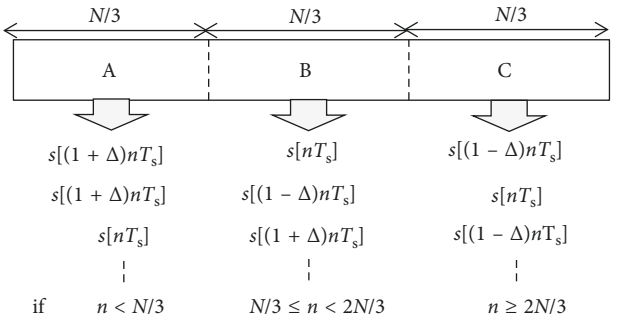

Figure 6: OFDM block with Doppler shift patterns.

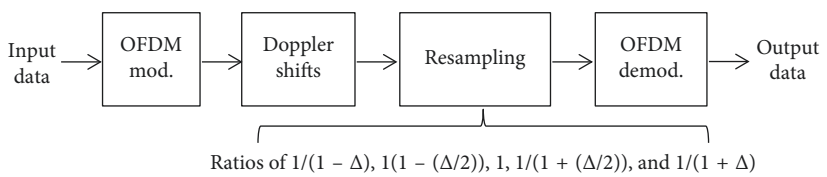

Figure 7: Resampling procedure.

Table 2: EVM results for various Doppler shift patterns and resampling ratios.

	Doppler shift patterns			Resampling ratio				
Case	A	B	C	$1/(1-\Delta)$	$1/(1-(\Delta/2))$	1	$1/(1+(\Delta/2))$	$1/(1+\Delta)$
(1)	Δ	0	$-\Delta$	76.9	36.1	36.3	90.0	128.8
(2)	Δ	$-\Delta$	0	131.8	83.1	35.1	32.6	80.3
(3)	0	Δ	$-\Delta$	137.5	160.8	47.4	29.9	60.0
(4)	0	$-\Delta$	Δ	154.3	122.3	68.0	57.2	103.1
(5)	$-\Delta$	Δ	0	197.2	149.1	119.6	62.1	29.9
(6)	$-\Delta$	0	Δ	188.8	163.6	71.4	21.8	32.2

Table 3: BER results Doppler shift patterns and resampling ratios.

	Doppler shift patterns			Resampling ratio				
Case	A	B	C	$1/(1-\Delta)$	$1/(1-(\Delta/2))$	1	$1/(1+(\Delta/2))$	$1/(1+\Delta)$
(1)	Δ	0	$-\Delta$	0.06	0.002	0.002	0.02	0.1
(2)	Δ	$-\Delta$	0	0.2	0.05	0.002	0	0.03
(3)	0	Δ	$-\Delta$	0.3	0.08	0	0	0.01
(4)	0	$-\Delta$	Δ	0.3	0.1	0.02	0.008	0.05
(5)	$-\Delta$	Δ	0	0.4	0.3	0.1	0.02	0
(6)	$-\Delta$	0	Δ	0.3	0.2	0.03	0	0

The average Doppler shift becomes zero for all Doppler shift patterns because the OFDM block length does not change. It indicates that resampling is not needed in the conventional approach. However, the appropriate resampling ratios having the lowest EVM and BER depend on Doppler shift patterns. If these Doppler shift patterns are known, the appropriate resampling ratios can be determined according to the results in Tables 2 and 3. Actual Doppler shift patterns are much complex and cannot be prospected.

The conventional approach takes the Doppler average in determining a resampling ratio. It induces the mismatch between determined and appropriate resampling ratios in the presence of large Doppler fluctuation. We take another approach to grasp the Doppler fluctuation, inserting a continuous wave (CW) into the OFDM frame to observe short-term Doppler shifts. The block diagram of CW-aided Doppler estimation is illustrated in Figure 8. The CW signal of $\sin(2\pi f_{\mathrm{CW}} t)$ and the OFDM transmitted signal are multiplexed in frequency. The CW signal is allocated as one of the OFDM subcarriers, and frequency spacing between CW and OFDM is not required. The Doppler-affected CW signal is extracted by the bandpass filter. The short-term Doppler shifts can be measured by detecting phase offsets in IQ demodulation, where the observed Doppler shifts are plotted in Figure 8.

The statistical results based on short-term Doppler shifts are summarized in Table 4. The CW signal of 30 kHz is added into the OFDM block in Figure 6. When we look into the results of average, standard deviation, maximum, and minimum values, the standard deviation gives useful information. These standard deviation values are close to the Doppler fluctuation of 10 Hz. The phenomena that the average values do not become zero would be caused by sudden changes in Doppler shifts. Doppler dispersion provides useful information to grasp large Doppler fluctuation.

4. Parallel Resampling

As reported in Section 3, it is difficult to find an optimal resampling ratio even for the simple Doppler shift patterns given by three sections if their Doppler shift patterns are unknown. Doppler shift patterns should be assumed as almost unknown for actual Doppler fluctuation caused by the irregular motions of transmitter or receiver units. We consider statistical information in short-term Doppler shifts and present a parallel resampling technique that a resampling range is extended by measured Doppler dispersion.

The conceptions of single and parallel resampling techniques are compared in Figure 9. The single resampling technique, regarded as a conventional method, determines a resampling ratio according to the Doppler mean. As long as the Doppler shift is time invariant, the single resampling can provide adequate performance for Doppler compensation. However, it cannot cope with Doppler fluctuation especially for the case that Doppler shift patterns are unknown. The parallel resampling technique uses both Doppler mean and standard deviation and extends the resampling range. The optimal resampling ratio is detected by checking all outputs in the extended resampling units (called as branches); i.e., the exhaustive search is adopted. The details of the exhaustive search are explained by the following receiver structure.

The block diagram of the parallel resampling receiver is illustrated in Figure 10. The CW and OFDM signals are multiplexed across the communication frame in the transmitter side (Figure 10(a)). As shown in Figure 8, we have improved the frequency allocation of CW and OFDM that the CW is regarded as one of the OFDM subcarriers. Their frequency bands are 30 kHz and 30 kHz to 60 kHz, respectively. Our previous work required frequency spacing, where CW and OFDM are allocated in 45 kHz and 50 kHz to 60 kHz [10]. In the receiver side (Figure 10(b)), the CW signal is separated by the bandpass filter. The Doppler

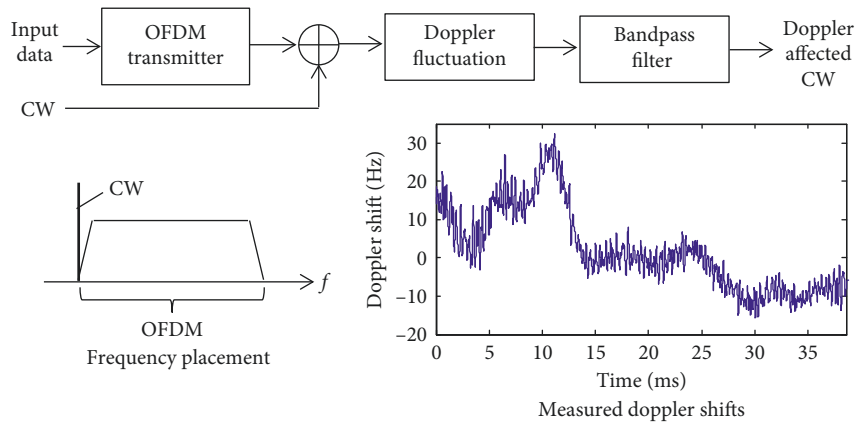

Figure 8: Block diagram of CW-aided Doppler estimation.

Table 4: Statistical results based on short-term Doppler shifts.

	Doppler shift patterns			Estimated Doppler shift (Hz)			
Case	A	B	C	Ave.	Std.	Max.	Min.
(1)	Δ	0	$-\Delta$	1.8	10.5	32.4	−15.7
(2)	Δ	$-\Delta$	0	4.9	12.5	44.1	−15.9
(3)	0	Δ	$-\Delta$	2.9	9.9	29.8	−15.4
(4)	0	$-\Delta$	Δ	3.3	13.1	49.6	−15.9
(5)	$-\Delta$	Δ	0	7.0	12.9	48.9	−20.7
(6)	$-\Delta$	0	Δ	4.4	10.2	43.0	−20.7

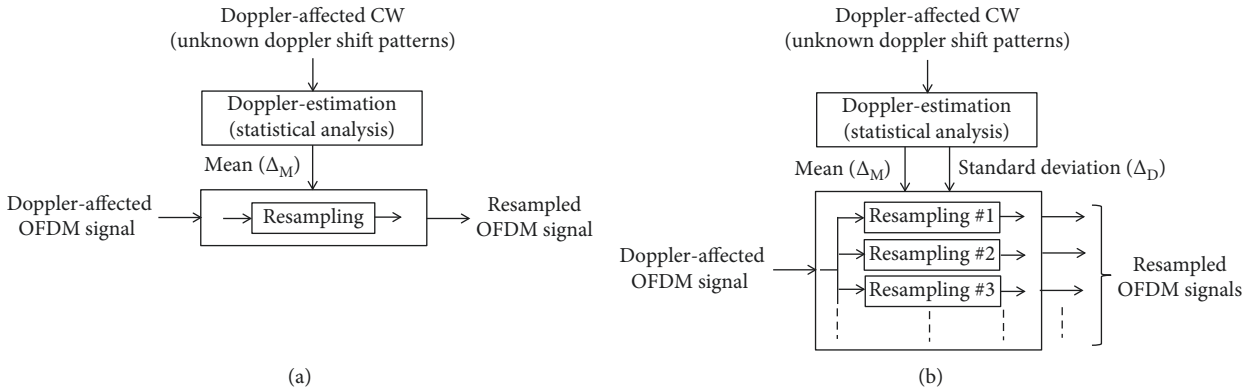

Figure 9: Conceptions of single and parallel resampling techniques. (a) Single resampling and (b) parallel resampling.

estimation unit calculates the mean and standard deviation values (Δ_M and Δ_D) from the measured short-term Doppler shifts. According to the values of Δ_M and Δ_D, the resampling range is extended as $1/(1-\Delta_M-\Delta_D), \ldots, 1/(1+\Delta_M), \ldots, 1/(1+\Delta_M+\Delta_D)$.

The receiver takes multiple branches for resampling and OFDM demodulation blocks, where every branch has a different resampling ratio. As mentioned in Section 3, the appropriate resampling ratio depends on Doppler shift patterns. For unknown shift patterns, it is very difficult to find the appropriate resampling ratio by only evaluating the received signals before OFDM demodulation. We apply the exhaustive search to cope with this problem. The parallel resampling receiver performs data checking for the outputted bit data after OFDM demodulation and selects the best branch having no data error. In the transmitter side, cyclic redundancy check (CRC) codes are inserted in bit data before forward error correcting (FEC) coding. In the receiver side, all branches are checked whether their outputted data have an error or not. The best branch having no error is selected, which corresponds to selecting the appropriate resampling ratio. If all branches have data errors, the final data are generated by merging all decoded data of branches in the bit level. The overhead of CRC codes might be counted. The overhead would be very small as far using CRC-16 or CRC-8.

The procedure of OFDM demodulation is shown in Figure 10(c), which is adopted in typical OFDM systems.

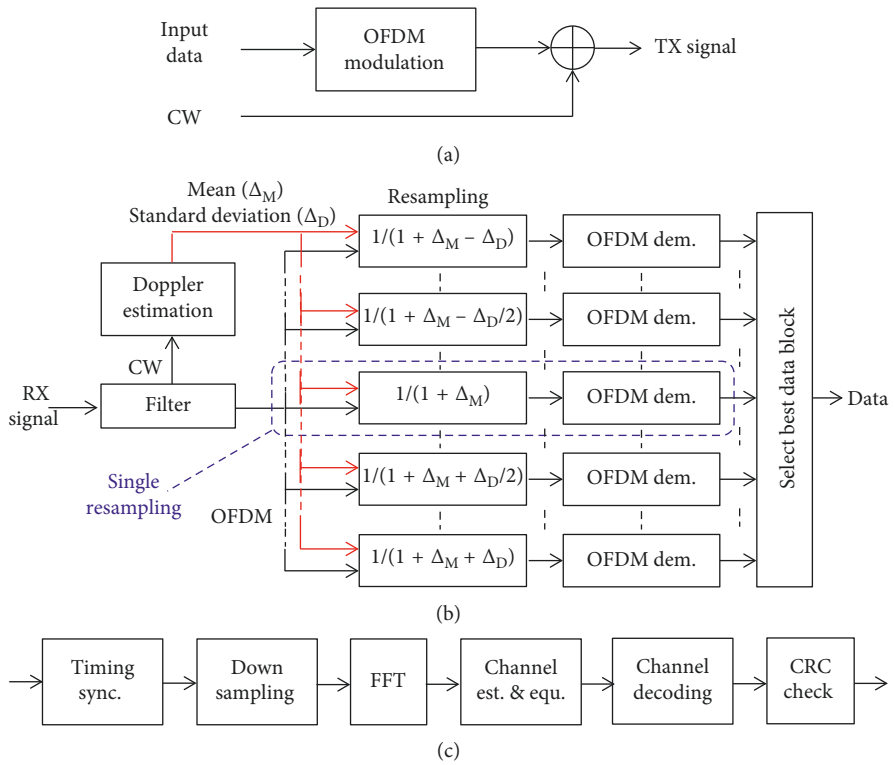

Figure 10: Block diagram of parallel resampling receiver. (a) Transmitter, (b) receiver, and (c) OFDM demodulation.

The single resampling is highlighted by the dashed lines in Figure 10(b), where the resampling ratio is given by $1/(1+\Delta_M)$ according to the Doppler mean value Δ_M. The performance comparison of single and parallel resampling techniques is reported in Section 5.

We mention examples of resampling range and number of branches in parallel resampling. Table 5 shows the examples of resampling ratios and number of branches (N_P). We express the resampling ratio by an integer format as

$$\frac{1}{1+\Delta_M+\Delta_D} = \frac{R}{R+\Delta_M+\Delta_D}, \quad (5)$$

where R relates the resolution of resampling as explained in Section 2. When we set $R = 10000$, and $\Delta_M = 0$, the resampling ratio becomes $10000 : 10000 + \Delta_D$ as an integer ratio. Note that the parameter of R depends on the Doppler tolerance. We set it according to the Doppler test results in Section 2. For the Doppler standard deviation value of 5 Hz (with zero mean), the parallel resampling receiver takes three branches whose ratios are 10000 : 9999, 10000 : 10000, and 10000 : 10001. It indicates that parallel resampling has a trade-off between improving communication performance and increasing computational complexity.

The number of branches has been fixed as $N_P = 11$ based on the empirical data in our acoustic communication tests in our previous work [10]. This paper applied the dynamic control of branches (we call it variable branches) in order to reduce computational complexity. The procedure for the variable branches is explained as follows:

Table 5: Examples of resampling ratios and number of branches.

Doppler std. ($\Delta_D f_C$) (Hz)	Resampling range (10000:m)	Number of branches (N_P)
5	(9999, 10000, 10001)	3
10	(9998, 9999, . . ., 10002)	5
20	(9996, 9997, . . ., 10004)	9

(a) Cut out a received signal for a certain frame

(b) Calculate Δ_M and Δ_D from the extracted CW

(c) Determine N_P according to Δ_D

Since the resampling ratio is adjusted by the unit of 1/10000, the target signal for resampling should hold at least 10000 samples. For example, the numbers of samples per frame amount from 10,000 to 100,000 for 200 kHz sampling frequency and 1024 subcarriers. It is advantageous to perform both resampling and statistical analysis of Doppler mean and standard deviation for the entire frame. The calculation of standard deviation for every frame is required for the variable branches. Its computational cost is $O(3N)$, which is much smaller than resampling processing itself given by $O(20N^2)$ (N denotes the number of samples per frame).

When the magnitude of Doppler fluctuation changes as time goes, the complexity reduction is available by changing the number of branches for each frame.

5. Experimental Results

We conducted the communication experiment on November 2017 in Mombetsu Port, Hokkaido, Japan. The

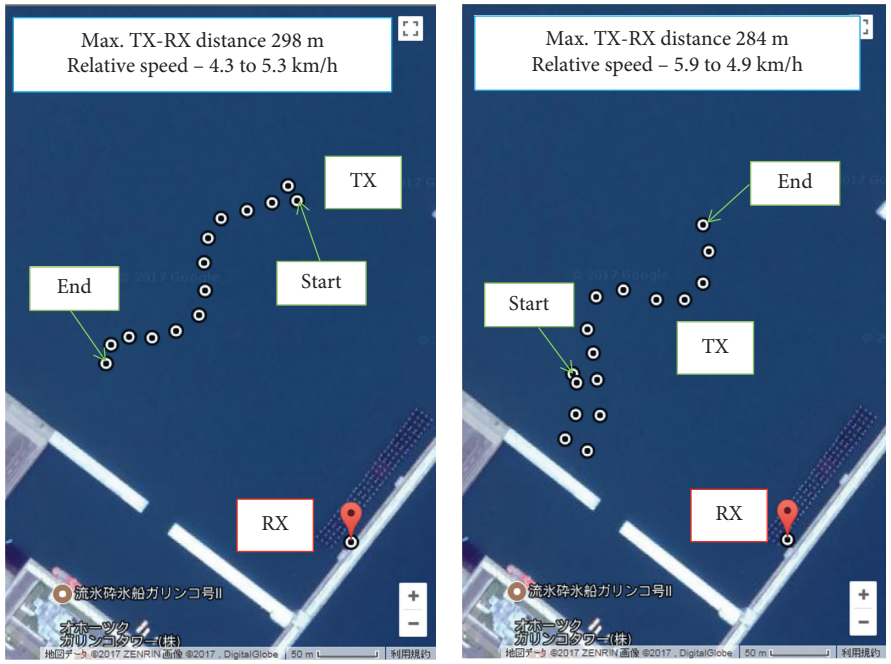

(a) (b)

Figure 11: Locations of transmitter and receiver units on Google Maps [12]. (a) Test 1 and (b) Test 2.

locations of transmitter (TX) and receiver (RX) units are plotted on aerial photograph in Figure 11. The sea depth was about 10 m. The receiver was fixed at 2 m below the sea surface. The TX unit was located at 1 m below the surface and moved by a ship with meandering trajectory. The average ship' speeds were about 3.7 km/h (2 knot) and 5.6 km/h (3 knot) in Test 1 and Test 2. The relative Doppler speeds between TX and RX units are not the same as the ship speeds because the directions of the ship do not agree with those of sound propagation.

The measured delay profile at the RX unit is plotted in Figure 12. The cluster of large delay waves is observed around 40 ms, inducing strong multipath interference. These delay waves are caused by the reflection of sea surface, bottom, and two side walls near the RX unit. Table 6 enumerates the experimental parameters. Due to the severe conditions on Doppler and multipath, the transmit data rate was set to 3 kbps. We have compared communication performance in single and parallel resampling techniques.

The results of carrier-to-noise ratio (CNR) and relative Doppler speed are reported in Figures 13 and 14 for Test 1 and Test 2. The horizontal axis denotes the frame number. We can observe Doppler fluctuation that the relative speed changes with plus or minus because the transmitter unit moves in the meandering trajectory as well as Figure 1(b). The CNR values are not uniform, which would be caused by the wave disturbance by a ship propeller and the ship direction.

The results of BER and number of branches (N_P) are plotted in Figures 15 and 16. We compared BER results in baseline (without resampling), single resampling, and parallel resampling (with fixed and variable branches). The results of BER = 0 are plotted on the line of BER = 10^{-4}.

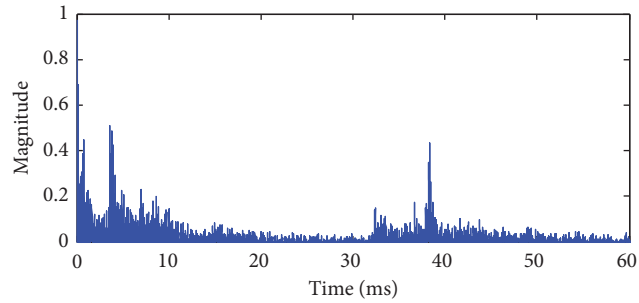

Figure 12: Delay profile at RX unit.

Table 6: Experimental parameters.

Modulation	QPSK-OFDM
Sampling frequency (kHz)	200
Center frequency (kHz)	45
Frequency band (kHz)	30 to 60
FFT size	1024
FFT length (ms)	34.1
GI length (ms)	4.3
Number of data subcarriers	512
Number of pilot subcarriers	512
Number of OFDM blocks	4
OFDM frame length (ms)	154
Frequency domain oversampling factor	2
FEC (coding rate)	Convolutional coding (1/2)
Transmit data rate (kbps)	3

The baseline degrades communication performance in the presence of Doppler, where most of frames have a larger BER close to 0.5. The single resampling can decrease BERs in

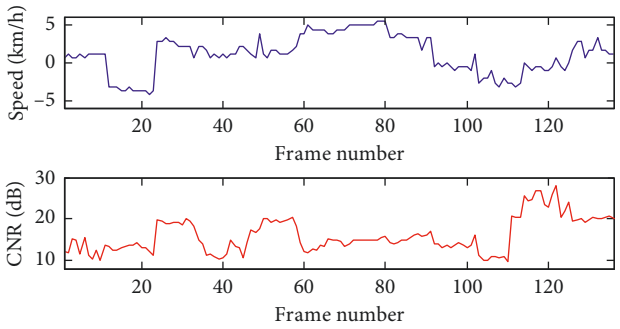

Figure 13: Results of CNR and relative Doppler speed in Test 1.

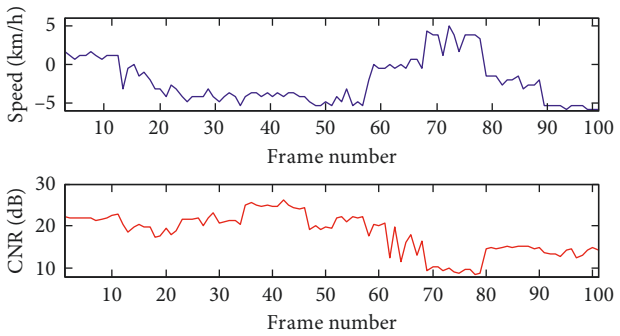

Figure 14: Results of CNR and relative Doppler speed in Test 2.

many frames, however, remains as bit errors in some frames. The parallel resampling has better BER performance than the baseline and single resampling. All communication frames are successfully demodulated in Test 1. Comparing fixed branches with variable branches in parallel resampling, their BER results are the same for all frames. The transitions of number of branches in the variable branches are also plotted in the graph. The number of branches changes for each frame, which indicates that the complexity reduction is available without sacrificing communication performance.

The measured Doppler shifts for the frame numbers of 33, 49, and 102 in Test 1 are shown in Figure 17. We can observe that the Doppler shift fluctuates with plus or minus within an OFDM frame as mentioned in Section 3. The BERs for the frame numbers of 33, 49, and 102 are 0.17, 0.45, and 0.37 in single resampling and all zeros in parallel resampling. Their results indicate that parallel resampling can improve communication performance under actual Doppler fluctuation.

Table 7 shows the summary of experimental results. The overall results of frame error rate (FER) are 0.096 and 0.24 for the single resampling in Test 1 and Test 2. The parallel resampling achieves FERs of 0 and 0.10. The parallel resampling with the variable branches saves computational cost by 28% to 33% compared with the fixed branches.

The parallel resampling has improved communication performance for large Doppler fluctuation; however, it relies on the exhaustive search with low computation efficiency. The further complexity reduction should be considered as a future issue. One of the key ideas is use of compressing sensing (CS). CS-based channel estimation in OFDM has

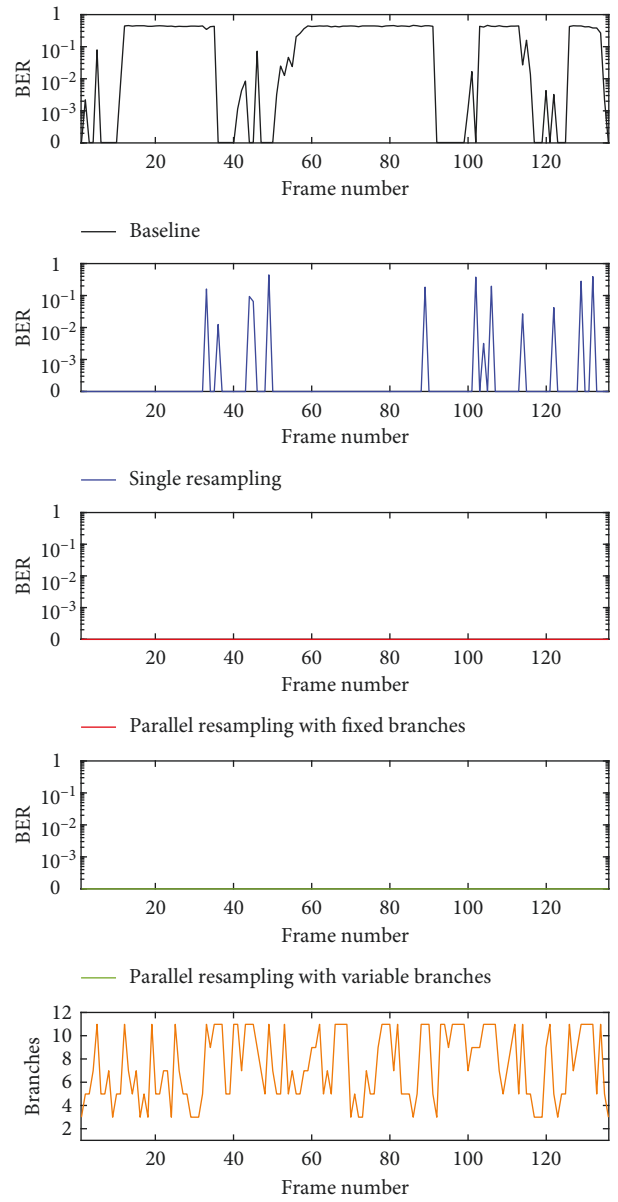

Figure 15: Results of BER and number of branches in Test 1.

been discussed in [13]. In UAC, a doubly spread acoustic channel (dispersion in time and frequency) is estimated by orthogonal matching pursuit (OMP) algorithm in [14, 15], which makes use of the sparse structure of channel impulse response. If Doppler fluctuation could be accurately estimated by the similar approach, an optimal resampling ratio is detected without the exhaustive search. Since the computational cost of OMP algorithm is much higher than that of Doppler mean and standard deviation, we would have to compare the overall complexity including Doppler estimation, resampling, and demodulation.

6. Conclusion

This paper improved a resampling technique for large Doppler fluctuation in underwater acoustic communication.

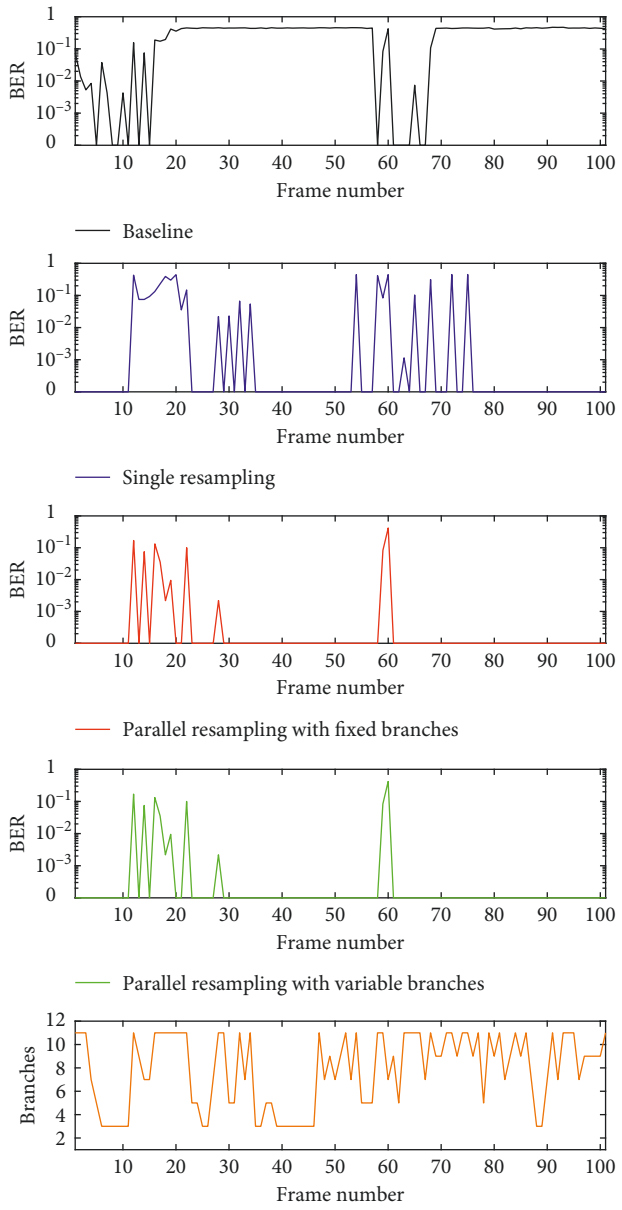

Figure 16: Results of BER and number of branches in Test 2.

The influence of Doppler fluctuation has been investigated by giving unknown Doppler shift patterns. According to the observation that Doppler dispersion gives useful information to grasp Doppler fluctuation, we have presented the parallel resampling technique that the resampling range is extended according to the measured Doppler deviation. The effectiveness of parallel resampling has been confirmed by evaluating communication performance comparing with single resampling.

The complexity reduction has been done by applying the variable branches in the parallel resampling receiver. It saves computational cost by 30 % compared with the fixed branches. However, its computation cost remains rather high compared with the single resampling. The further complexity reduction will be studied in our future work.

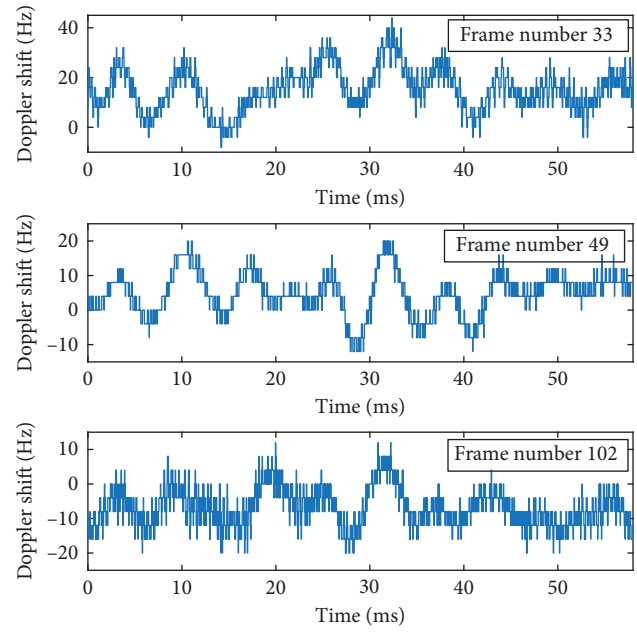

Figure 17: Measured Doppler shifts for frame numbers of 33, 49, and 102 in Test 1.

Table 7: Summary of experimental results.

	Single resampling		Parallel resampling with fixed branches [10]		Parallel resampling with variable branches (this work)	
	Test 1	Test 2	Test 1	Test 2	Test 1	Test 2
FER	0.096	0.24	0	0.10	0	0.10
Number of branches (N_P)	1	1	11	11	7.4	7.9

Data Availability

The experimental and simulation data used to support the findings of this study are included within the article.

Conflicts of Interest

The authors declare that there are no conflicts of interest regarding the publication of this paper.

Acknowledgments

The authors would like to thank Dr. Hiroshi Tanimoto for their support and assistance with this project. This work was supported by the City of Mombetsu, Mombetsu Okhotsk Tower, and JSPS KAKENHI (Grant Number 16K18099).

References

[1] M. Stojanovic, "Low complexity OFDM detector for underwater acoustic channels," *IEEE Oceans*, pp. 18–21, 2006.

[2] S. Yoshizawa, H. Tanimoto, and T. Saito, "Data selective rake reception for underwater acoustic communications in strong

multipath interference," *Journal of Electrical and Computer Engineering*, vol. 2017, Article ID 5793507, 9 pages, 2017.

[3] B. S. Sharif, J. Neasham, O. R. Hinton, and A. E. Adams, "A computationally efficient Doppler compensation system for underwater acoustic communications," *IEEE Journal of Oceanic Engineering*, vol. 25, no. 1, pp. 52–61, 2000.

[4] B. Li, S. Zhou, M. Stojanovic, L. L. Freitag, and P. Willett, "Multicarrier communication over underwater acoustic channels with nonuniform Doppler shifts," *IEEE Journal of Oceanic Engineering*, vol. 33, no. 2, pp. 198–209, 2008.

[5] K. Tu, T. M. Duman, M. Stojanovic, and J. G. Proakis, "Multiple-resampling receiver design for OFDM over Doppler-distorted underwater acoustic channels," *IEEE Journal of Oceanic Engineering*, vol. 38, no. 2, pp. 333–346, 2013.

[6] S. Beygi and U. Mitra, "Optimal Bayesian resampling for OFDM signaling over multi-scale multi-lag channels," *IEEE Signal Processing Letters*, vol. 20, no. 11, pp. 1118–1121, 2013.

[7] Z. Wang, S. Zhou, G. B. Giannakis, C. R. Berger, and J. Huang, "Frequency-domain oversampling for zero-padded OFDM in underwater acoustic communications," *IEEE Journal of Oceanic Engineering*, vol. 37, no. 1, pp. 14–24, 2012.

[8] T. Ebihara and G. Leus, "Doppler-resilient orthogonal signal-division multiplexing for underwater acoustic communication," *IEEE Journal of Oceanic Engineering*, vol. 41, no. 2, pp. 408–427, 2016.

[9] A. E. Abdelkareem, B. S. Sharif, C. C. Tsimenidis, and J. A. Neasham, "Compensation of linear multiscale Doppler for OFDM-based underwater acoustic communication systems," *Journal of Electrical and Computer Engineering*, vol. 2012, Article ID 139416, 16 pages, 2012.

[10] S. Yoshizawa, H. Tanimoto, T. Saito et al., "Parallel resampling receiver for underwater acoustic communication with non-uniform Doppler shifts," *IEEE Oceans–Anchorage*, p. 4, 2017.

[11] C.-H. Hwang, K.-M. Kim, S.-Y. Chun, and S.-K. Lee, "Doppler estimation based on frequency average and remodulation for underwater acoustic communication," *International Journal of Distributed Sensor Networks*, vol. 2015, Article ID 746919, 2015.

[12] https://www.google.com/permissions/geoguidelines.html.

[13] Y. Zhang, R. Venkatesan, O. A. Dobre, and L. Cheng, "Novel compressed sensing-based channel estimation algorithm and near-optimal pilot placement scheme," *IEEE Transaction on Wireless Communication*, vol. 15, no. 4, pp. 2590–2603, 2016.

[14] W. Li and J. C. Preisig, "Estimation of rapidly time-varying sparse channels," *IEEE Journal of Oceanic Engineering*, vol. 32, no. 4, pp. 927–939, 2007.

[15] F. Qu, X. Nie, and W. Xu, "A two-stage approach for the estimation of doubly spread acoustic channels," *IEEE Journal of Oceanic Engineering*, vol. 40, no. 1, pp. 131–143, 2015.